CivilEng

MDPI

Article

Rejuvenation Mechanism of Asphalt Mixtures Modified with Crumb Rubber

Hossein Noorvand [1,*], Kamil Kaloush [1], Jose Medina [1] and Shane Underwood [2]

[1] School of Sustainable Engineering and the Built Environment, Arizona State University, P.O. Box 873005, Tempe, AZ 85287-3005, USA; Kamil.Kaloush@asu.edu (K.K.); jrmedina@asu.edu (J.M.)
[2] Department of Civil, Construction, and Environmental Engineering, North Carolina State University, Raleigh, NC 27695-7908, USA; bsunderw@ncsu.edu
* Correspondence: hnoorvand@asu.edu; Tel.: +1-(480)-300-1919

Abstract: Asphalt aging is one of the main factors causing asphalt pavements deterioration. Previous studies reported on some aging benefits of asphalt rubber mixtures through laboratory evaluation. A field observation of various pavement sections of crumb rubber modified asphalt friction courses (ARFC) in the Phoenix, Arizona area indicated an interesting pattern of transverse/reflective cracking. These ARFC courses were placed several years ago on existing jointed plain concrete pavements for highway noise mitigation. Over the years, the shoulders had very noticeable and extensive cracking over the joints; however, the driving lanes of the pavement showed less cracking formation in severity and extent. The issue with this phenomenon is that widely adopted theories that stem from continuum mechanics of materials and layered mechanics of pavement systems cannot directly explain this phenomenon. One hypothesis could be that traffic loads continually manipulate the pavement over time, which causes some maltenes (oils and resins) compounds absorbed in the crumb rubber particles to migrate out leading to rejuvenation of the mastic in the asphalt mixture. To investigate the validity of such a hypothesis, an experimental laboratory testing was undertaken to condition samples with and without dynamic loads at high temperatures. This was followed by creep compliance and indirect tensile strength testing. The results showed the higher creep for samples aged with dynamic loading compared to those aged without loading. Higher creep compliance was attributed to higher flexibility of samples due to the rejuvenation of the maltenes. This was also supported by the higher fracture energy results obtained for samples conditioned with dynamic loading from indirect tensile strength testing.

Keywords: crumb rubber; asphalt mixtures; rejuvenation; swelling; aging; dynamic load; creep compliance; indirect tensile strength

1. Introduction

Asphalt has been preferential choice in pavement construction because of its effectiveness and practicality; however, as other organic substances, it is also subjected to the aging phenomenon. Asphalt aging is one of the main factors causing pavements deterioration and cracking. Asphalt becomes fragile and brittle due to exposure to oxygen, heat, and ultraviolet (UV) light. This process begins during asphalt mixture construction and continues through progressive oxidation of the in-place material in the field. It ultimately reduces the durability of flexible pavements [1,2]. It is also reported that such phenomenon can have a positive effect on the rutting resistance of asphalt pavements [3,4]. Therefore, aging has a significant impact on the road durability and long-term performance.

Aging of asphalt has been mainly characterized in three phases: unaged, short-term aged, and long-term aged conditions [5]. Short-term aging is associated with the asphalt mixtures preparation at high temperatures and continues during the construction phase. The loss of volatile compounds in the binder further hardens the asphalt mixtures in the field. Long-term aging continues throughout the service life of pavements, which in turn depends on several

other external factors such as traffic loading, temperature, and environmental parameters [6,7]. In general, asphalt is composed of asphaltenes, resins, saturates, and aromatics, and it has been suggested that the asphaltene fraction plays a significant role in the chemical analysis of aging in asphalt binders [8]. Asphaltenes are insoluble when the asphalt binder is dissolved in a nonpolar solvent such as pentane, hexane, or heptane. The collective name for the components that dissolve in these solvents is maltenes, which is comprised of resins and oils. Therefore, with loss of volatile components and exudation of oily components during aging process, asphalt pavement performance is deteriorated, which results in the reduction of asphalt resistance to cracking [9].

1.1. Subsection Crumb Rubber Modified Asphalt

Approximately 850 million to 3 billion tires are disposed of in landfills, stockpiled, or illegally dumped around the United States, a number that rises by 250 million tires every year [10]. The disposal of these scrap tires has been a serious issue due to many reasons such as lack of landfill space, environmental issues, etc. Therefore, the utilization of crumb rubber, derived from tires, has long been supported by environmental and government agencies to decrease the disposal problem linked with waste tires [11]. The road industry has the potential to consume part of the disposed scrap tires and using it in asphalt binders. Previous studies have shown that crumb rubber modified (CRM) asphalt binders can improve physical and rheological properties of asphalt mixtures including reduction of thermal reflective cracking and traffic noise, increased resistance to rutting and fatigue cracking, and improved aging and oxidation resistance [12–16]. Therefore, there is an increasing interest in utilizing CRM binders in hot mix asphalt (HMA) pavements in in the United States and other countries around the world [17].

1.2. Problem Statement and Objective

A field observation of various pavement sections of crumb rubber modified asphalt-rubber friction courses (ARFC) on freeways near Tempe, Arizona, has shown an interesting pattern of transverse/reflective cracking. These ARFC overlays were placed several years ago on existing jointed plain concrete pavement (JPCP) to mitigate the noise from vehicles. Over the years, the shoulders had very noticeable and extensive cracking over the joints; however, the center lane of the pavement showed less cracking in terms of both severity and extent. Figure 1 shows the ARFC overlays and the cracking pattern associated with reflective cracking. The entire ARFC overlay (including shoulders and traveling lanes) is made of the same ARFC material, constructed around 2010 over the JPCP pavement. A closer look at the crack pattern of the pavement shows that the shoulders have higher severity of cracking compared with the center/driving lanes of the road, which has been frequently subjected to traffic loadings. The effect of crack opening severity is also evident in the center lane where some parts of the lane (wheel path) are more frequently exposed to traffic as seen in Figure 2.
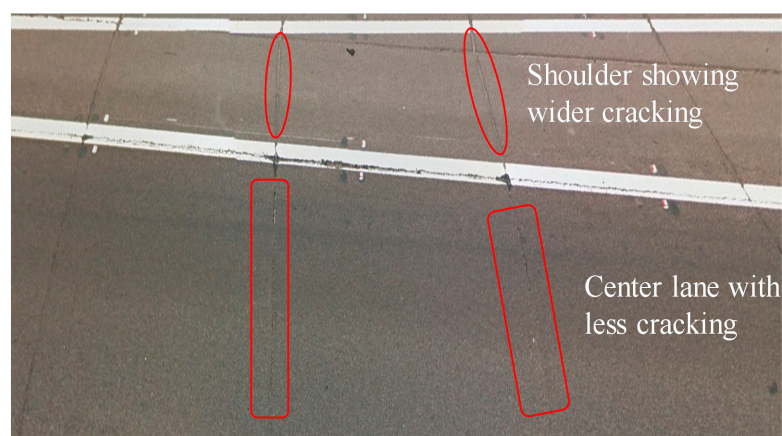

Figure 1. Crack severity comparison between shoulder and driving lane (source: map-highway 101, Tempe Arizona).
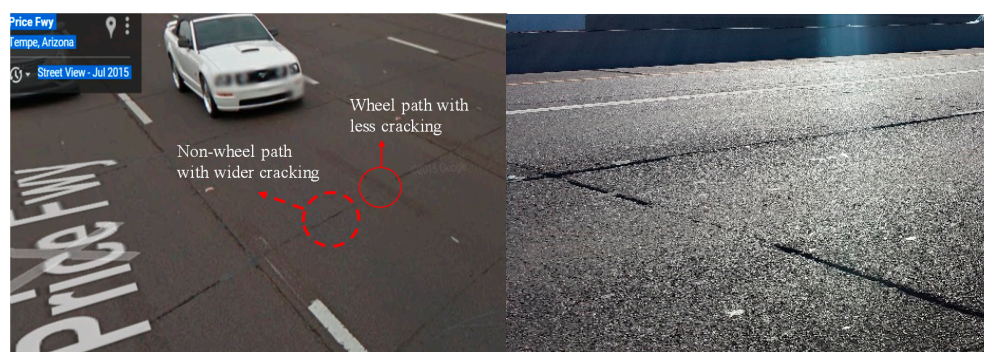
Figure 2. Severity of crack opening comparison in the driving lane between wheel path and non-wheel path (source: left photo Google map-highway 101, Tempe Arizona; right photo captured while driving on highway 202, Tempe, Arizona).

Several studies have reported that rubber particles swell by the absorption of the bitumen oily components (aromatic oils and resins) at high blending temperatures (160–220 °C) to form a gel-like material [18–20]. Figure 3 illustrates a schematic swelling mechanism of rubber particles when reacted with asphalt binder. CRM Asphalt binder is made by blending and reacting hot asphalt binder at about 190 °C with rubber particles. Crumb rubber particles are added to the hot binder at the ambient temperature and thoroughly mixed (Stage 1). During the heating and mixing of the asphalt and the rubber, the rubber particles swell as shown in Figure 3 (Stage 2) that alters the resultant mixture to a gel-like material.

It has been shown that asphalt binders modified with crumb rubber generally absorbs low molecular weight maltenes and leave the residual asphalt binder containing a higher proportion of asphaltene [20–23]. Thus, during this reaction there is a decrease of the oily fraction and at the same time an increase of rubber particle sizes which follows with reducing the inter-particle distance [20,22]. It is reported that particles of crumb rubber could swell by a factor of 3–5 compared with their original size [21,22]. Considering such phenomenon in the field observation, it maybe be hypothesized that the lighter asphalt fraction (oil and resins) absorbed by rubber particles during mix production, migrate out into the asphalt mastic over time. Such mechanism contributes to the rejuvenation of the ARFC pavement layer over time, and hence reduces the crack severity and growth resulting from aging. This might explain why there is less severity of cracking on the driving lane particularly the part exposed to wheel path compared with the shoulders and the part of trafficked lane that subject to no or little loading. The objective of this study is to first study the swelling mechanism of rubber particle and then capture and quantify this hypothetical rejuvenation mechanism noted earlier in a laboratory setting.
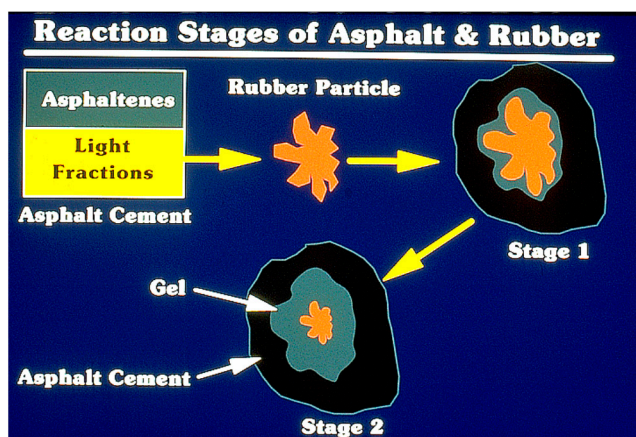

Figure 3. Swelling mechanism of rubber [23].

2. Experimental Program

2.1. Materials

A gap graded asphalt rubber mixture produced by Granite Construction for a Sacramento County project was available for the laboratory evaluation. The plant mixture, designated as RHMA-G 19 mm Superpave mix design, was produced at Vernalis plant in California with the nominal maximum aggregate size of 19 mm, binder content of 7.5%, and the base binder grade of PG 64-16. The percentage of the crumb rubber modifier was 18% by weight of asphalt rubber binder. The mix design gradation is given in Table 1. Also, the maximum theoretical specific gravity (Gmm) and voids in mineral aggregate, VMA, (%) were given as 2.362 and 19.7, respectively.

Table 1. Mix gradation.

Sieve Size (mm)	25	19	12.5	9.5	4.75	2.36	1.18	0.6	0.3	0.15	0.075
Passing (%)	100	98	83	65	30	16	11	8	6	4	2.6

2.2. Sample Preparation

Samples were received in 19 L metal pails. At the Arizona State University laboratory, the mixtures were removed from the pail by heating them at 135 °C for 90 min. Random samples were taken from multiple pails and combined into cloth bags with enough mass to make one gyratory sample each. The mixtures were prepared using a Superpave gyratory compactor to fabricate samples with 120 mm in height and 150 mm in diameter. After that, samples were cut to discs 40 mm in height and 150 mm in diameter. Two replicates were obtained from each compacted gyratory sample. The target air void of the specimens was in the range of 5–5.5%. The air void measurement followed AASHTO T 166 and AASHTO T 166.

2.3. Swelling Testing

The swelling of the crumb rubber particles was studied by using crumb rubber particles retained on the 0.420 mm and the 0.297 mm sieves. These particles were chosen since they represented the two largest particle sizes by mass of the crumb rubber blend. Then, each size of rubber particles (0.420 and 0.297 mm) was blended with three different grades of asphalt binder: a PG 70-10, PG 64-22, and PG 58-22. Next, a scanning electron microscope (SEM) technique was performed on crumb rubber particles before and after blending with asphalt binder. For preparation of the un-mixed samples (before blending), particles were first sprinkled onto SEM holders for imaging. During this process it was ensured that particles were not touching one another, and imaging could sufficiently capture the characteristics of single particles. After that, single size particles were mixed for 30 min with each asphalt binder at a temperature of 170 °C, and a volume content of 8.7%. Such a volume content was selected in order to prevent the SEM samples from being too crowded with particles of rubber, which would have significantly complicated the image analysis. To determine swelling, a sample of each of the three rubberized asphalt cements were smeared onto the SEM holders in thin films. Smearing the samples onto the holders allows the particles to be exposed and easily identified. It should also be noted that images were taken before and after mixing with asphalt using a SEM-XL30 environmental microscope under the following conditions: environmental mode, secondary electron signal, and accelerating voltage of 15 kV. For both the pre-blended and post-blending cases 35 SEM scans were taken in order to develop a probabilistic distribution of particle sizes.

2.4. Experimental Set-Up

After preparing the samples, a conditioning test protocol was designed to capture the hypothesized scenarios of the asphalt rubber pavement. While aging studies are mostly carried out based on binders rather than mixtures, several studies have also proposed accelerated laboratory aging test protocols for asphalt mixtures. For the compacted asphalt

mixtures, Strategic Highway Research Program (SHRP) has proposed a long-term oven aging process in which specimens are conditioned for 96 h at 85 °C [24]. The intention was to simulate the effects of aging of asphalt mixtures during their service life, for roughly 5 to 10 years [25]. Nonetheless, laboratory aging with long-term oven aging does not match field aging and can cause inaccurate performance predictions [26]. Therefore, other researchers have developed alternative aging protocols by altering the conditioning time and/or oven temperature [27,28]. However, more recent developments have emphasized the necessity of other specific environmental conditions such as moisture, temperature, and UV radiation in order to simulate the aging of bituminous mixtures more realistically [29,30]. While the importance of aging protocol for compacted asphalt mixtures is recognized, this study followed the aging method per SHRP study as this study focused on simulating 'aging' in the sense of oxidation. Additionally, since the scope of this study required aging of the asphalt concrete specimens under dynamic loading, introducing other environmental conditions was not possible. Furthermore, a lower temperature was used for aging the mixture because it was a gap graded and external confinement (to prevent slumping during the aging protocol) was not available in order to minimize any possible damage on specimens during simultaneous aging and loading.

A UTM-25 environmental chamber was used for conditioning the specimens at a temperature of 60 °C and for 96 h. During conditioning, the two replicates were kept inside the chamber. One replicate was only exposed to the high temperature with no external loading and the other was subjected to a dynamic load as being aged during the conditioning procedure. Going back to the original problem statement the, the former represents what happens on the shoulders and the latter represents what happens in the driving lane of the pavement scenario. This aging conditioning setup is shown in Figure 4. One parameter which was considered before dynamic conditioning of the specimens was the unloading time, which represent the rest period. Typically, the loading and unloading time of the dynamic creep testing is 0.1 and 0.9 s, respectively. However, in this test, unloading time was increased to 5 s to allow for sufficient relaxation and (it was believed) to better represent the rest periods that might occur in an actual pavement. In addition, it should be noted that Haversine function was used as the mode of load application.
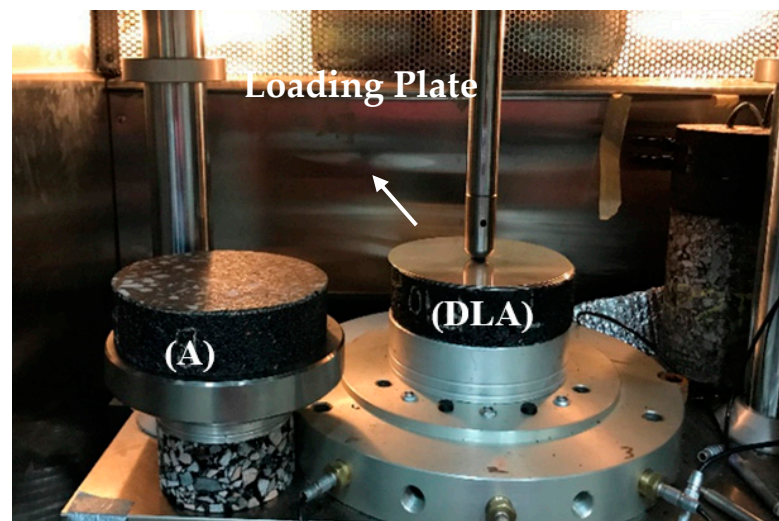

Figure 4. Conditioning method for aged (A) and dynamically loaded aged (DLA) specimens.

In an effort to prevent or minimize the damage to the DLA specimens, it was essential to determine the right magnitude of the dynamic loads that should apply on specimens for 95 h at 60 °C. It was necessary to have a loading of small amount not to damage the samples and at the same time it is sufficient to mobilize the oil from crumb rubber particles. After several trials, it was found that 0.8 kN was the appropriate value of load to be applied. Under this load, the accumulated strain increased up to 1.4% until 15,000 cycles, after that

it remained constant until 65,000 cycles. It was also recognized that using a loading plate on specimen was essential in order to distribute the loads across the entire contact surface of specimens during conditioning.

2.5. Testing Procedure

Aging changes the creep and relaxation behavior of the binder and its failure properties (21,22). So, to compare the effect of aging with and without dynamic load conditioning, creep compliance testing and indirect tensile strength (IDT) test were used per AASHTO T 322-07.

2.5.1. Creep Compliance

Creep compliance determines the time dependent strain of samples under constant load, and it is considered as a fundamental property of viscoelastic materials. Two buttons 50 mm apart in both the horizontal and vertical directions were glued on the two sides of each specimen, and linear variable displacement transducers (LVDTs) were installed to measure the horizontal and vertical strains (Figure 5). The measurements were obtained through a data acquisition system. After instrumentation, the specimens were kept inside an environmental chamber to reach the target temperature, which was 0 °C. Thermocouples were used to ensure that specimens reach the respective temperature, which took approximately 7 h. Once the sample reached at 0 °C, the creep load of 3–4 kN was adjusted to create a deformation in the range of 0.00125 to 0.0190 mm as specified by AASHTO T 322. The test was performed for 200 s. Three replicates were used for creep compliance tests.

Figure 5. Instrumentation of the specimens for creep compliance testing.

2.5.2. Indirect Tensile Strength Test

The IDT test is a part of the AASHTO T 322 test protocol. The main purpose of the test is to determine the tensile strength of asphalt mixtures. In this test, a specimen of 150 mm (6 in) diameter and not more than 63 mm (2.5 in) thickness is loaded at a constant rate of 50 mm/min (2.0 in/min) until it fails. After performing the creep compliance test, the LVDTs were removed, and the specimens were kept in the chamber to reach 10 °C at which point the test was performed (Figure 5). For this test, the primary interest is the tensile strength (S_t) value, which is obtained by using the measured peak load and Equation (1).

$$S_t = \frac{2P_f}{\pi \cdot D \cdot t} \tag{1}$$

where;

S_t = tensile strength (kPa),
P_f = failure load (KN),
t = specimen thickness (m), and
D = specimen diameter (m).

Other useful parameters such as the fracture energy can be calculated by determining the area under the load-vertical deformation curve. Two different facture energy parameters can be calculated: the fracture energy until failure (Γ_{fa}) and the total fracture energy (Γ_{ft}). The fracture energy until failure is defined as the area under the load-vertical deformation curve until maximum load occurs, while the total fracture energy is defined as the total area under the load-vertical deformation curve until the end of the test. Higher tensile strength and/or fracture energy means a higher crack resistance of the mixture [31].

3. Results

In this section, the findings from SEM image for swelling study, visual observation of the conditioned samples, creep compliance, and IDT test results are reported and discussed.

3.1. Swelling of Crumb Rubber

Figure 6 shows the typical SEM images of the pre- and post- blended rubber particles for the cases of PG 64-22. The principle of equivalent sphere diameter (*ED*) was used from the SEM images to estimate the particle size. This principle states that the volume occupied by a particle can be equated to the volume of a sphere that has a diameter determined by setting the 2D projected area of the particle to that of a circle and then solving for the needed diameter of the circle [32,33]. For this reason, the area of the particles highlighted in Figure 6 was used to estimate the *ED*. The area of 35 original individual rubber particles (unswelled) were determined by the built-in functionality of the ImageJ software together with Equations (2) and (3) to first approximate the *ED* and then measure the volume for each individual rubber particle.

$$ED = 2\sqrt{\frac{A}{\pi}} \tag{2}$$

$$V = \frac{4}{3}\pi\left(\frac{d}{2}\right)^3 \tag{3}$$

where;

ED = the equivalent diameter in mm,
A = the area of the particle in, mm^2, and
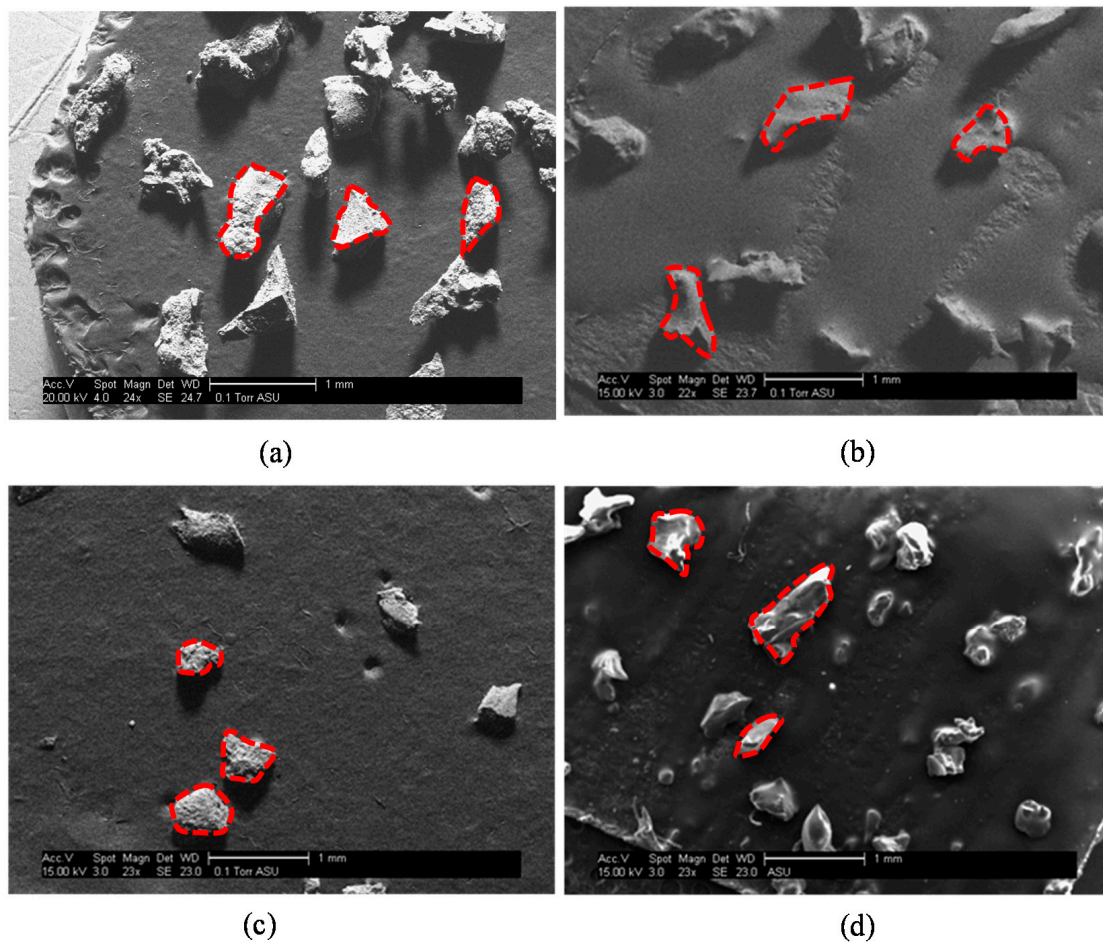*V* = the equivalent sphere volume in mm^3.

(a)

(b)

(c)

(d)

Figure 6. SEM images illustrating the (**a**) pre-blended and (**b**) post-blended 0.420 rubber particles, and the (**c**) pre-blended and (**d**) post-blended 0.297 mm rubber particles. (Adapted with permission from ref. [19], Copyright 2017 Elsevier).

It was found that the distribution of particle sizes was following standard Gaussian distribution, so a statistical distribution was obtained for the particles volume accordingly. Volume distribution for both the pre- and post-blended 0.420 mm and 0.297 mm rubber particles are illustrated in Figure 7a,b respectively. The analysis showed that the volume of 0.420 mm particles increased by 15%, 40%, and 24% for PG 70-10, PG 64-22, and PG 58-22, respectively. With respect to 0.297 mm particles, similar trend was observed where increase in volume was 17%, 47%, and 66%, respectively. For both particle sizes, it was observed that the PG 70-10 had the least amount of swelling since asphalt binders with higher stiffness are assumed to have smaller lighter fraction content, and thus there is less interaction between the rubber particles and the asphalt cement [19]. The PG 64-22 and PG 58-22 showed fairly inconsistent results (higher swelling for PG 64-22 with the larger particles and less swelling with the smaller particles). The contradictory results can be due to the possibility of particle breakdown/splitting during the processing [19].
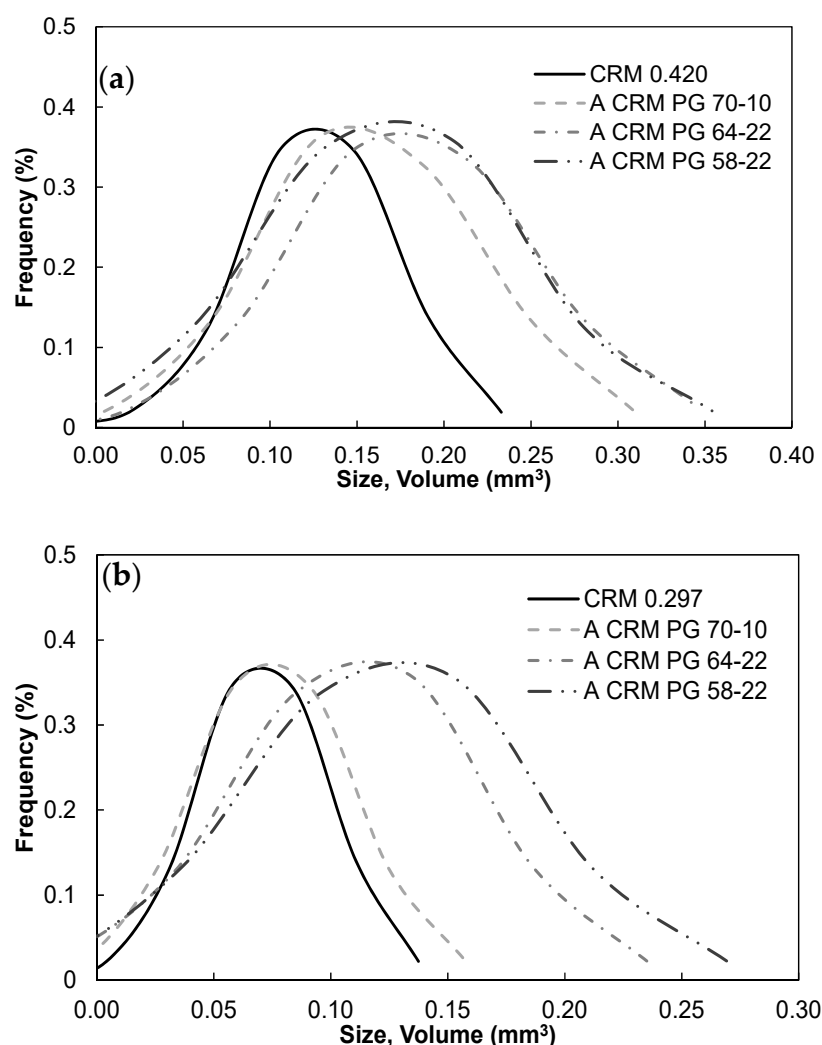
Figure 7. Particle volume distribution of both pre- and post-blended rubber particles retained on sieve (**a**) 0.420 mm and (**b**) 0.297 mm (*A CRM PG (70-10, 64-22, 58-22) represent the distribution of the post-blending particles). (Adapted with permission from ref. [19], Copyright 2017 Elsevier).

3.2. Characteristics of Conditioned Samples

After sample conditioning, the air voids of the various specimens were re-measured. Samples with no dynamic loading had an increase of about 1% in air voids; whereas the sample conditioned with dynamic loading had an air voids increase of about 1.5%. In general, the increase in air voids is somehow expected as the samples will go through a physical change due to the high temperature exposure without any confining media. However, what was encouraging is that the difference in the air voids between the two sets of samples (with and without dynamic loading) was small. In addition, changes on the specimens' surface were examined as shown in Figure 8. It was observed that the specimens exposed to conditioning had a darker surface shown in Figure 8b,c attributed to aging compared with control (Co) sample (Figure 8a). Comparing Figure 8b,c, aged sample under dynamic load (Figure 8c) showed a shinier surface compared with the samples subjected to only aging (Figure 8b).
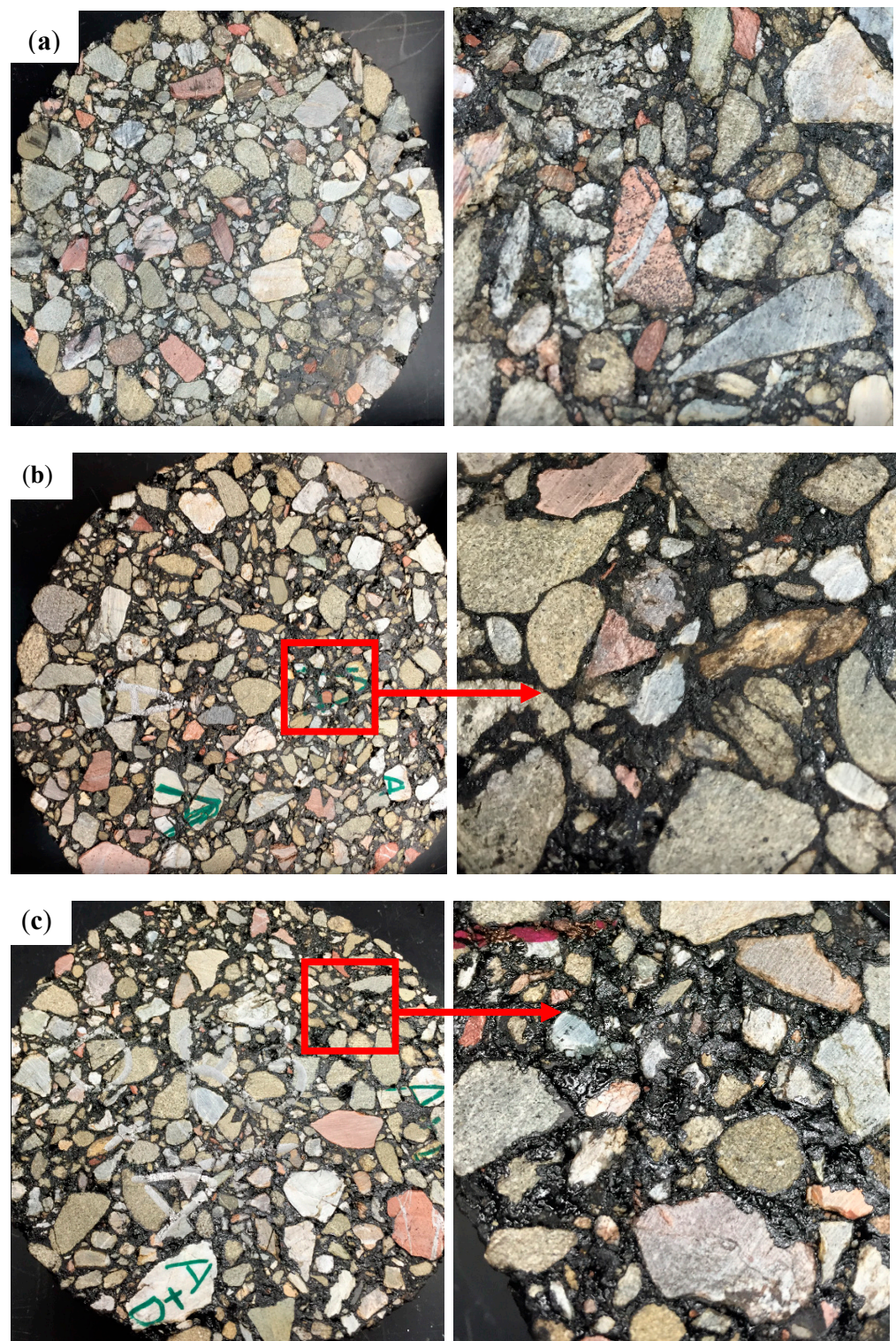
Figure 8. Surface characteristics photos of (**a**) Co sample, (**b**) aged sample, and (**c**) aged sample under dynamic load.

The shiny surface of the aged sample under dynamic load might be attributed to the presence of oils migrating out from crumb rubber particles over the conditioning period. This could be as result of bleeding. Such observation may corroborate the hypothesis of this study claiming that the oily compounds migrate out from crumb rubber particles upon exposing the pavement to traffic loads. It is also interesting to mention that the

same process was also applied to a conventional dense graded asphalt mixture, but the surface characteristics of both conditioned samples remained the same (no shiny or rich binder surface).

3.3. Creep Compliance

The average creep compliance for three replicates, each for the Co mixtures with no aging, aged mixtures (A) and aged mixtures under dynamic load (DLA) was calculated in general accordance with AASHTO T 322 and plotted in Figure 9. The creep compliance of all replicates, and for each designated mixture, had variability in the range of 5–20%. From the figure, it is evident that the aging process reduced the creep compliance of mixtures. In general, when asphalt is exposed to aging, it becomes stiffer over time and therefore it shows a lower degree of deformation. This is shown as lower creep compliance of aged samples compared with Co samples. An additional interesting trend can be observed; the aged mixtures subjected to dynamic loading showed higher creep compliance compared to the mixtures aged without loading. Again, this may provide further support to the hypothesis of this study which claims that crumb rubber swelled particles could provide rejuvenation to asphalt mixtures when subjected to loads. It was earlier observed that DLA samples had a shinier surface implying the higher portion of oil distributed throughout the mixture and the presence of oily compounds can hence provide more flexibility for specimen. Therefore, when creep compliance testing was performed, the higher flexibility of DLA samples resulted in higher creep compliance compared with the A samples.
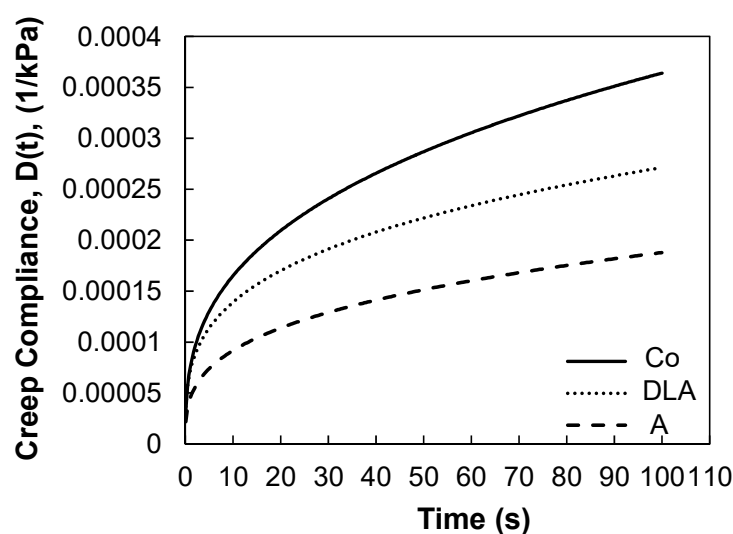

Figure 9. Average creep compliance of Co, A, and DLA samples.

Creep compliance data at 2.4, 5, 10, 20, 50, and 95 s for each mixture type are shown in Figure 10. An ANOVA and statistical *t*-test analysis were carried out at a 95% confidence level for creep compliance data at 2.4, 5, 10, 20, 50, and 95 s for each of the three replicates of the three mixtures: Co, A, and DLA. The ANOVA analysis was used to compare the difference between all means and evaluate the significance of the total differences; and the *t*-test was performed to compare individual cases of DLA and A to the Co specimens as well as individually between the A and DLA specimens. In all cases, the results indicated a statistical significance in the creep compliance values. The significance was more pronounced after 10 s of creep compliance testing.
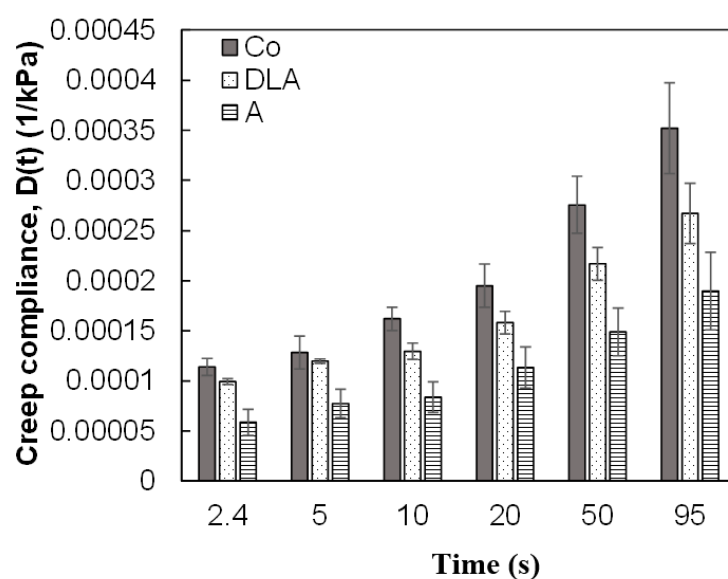
Figure 10. Creep compliance data for Co, A, and DLA samples at 2.4, 5, 10, 50, and 95 s3.4. Indirect Tensile Strength Test.

The IDT test results are shown in Figures 11 and 12. With respect to the unconditioned and conditioned mixes, the average strength values for Co replicates were greater than the conditioned samples (A and DLA). However, it was found that the strength of Co versus A and DLA specimens are not statistically significant at 90% level of confidence using ANOVA. Comparing energy parameters for the conditioned mixtures (DLA and A) with Co mix, it is seen that average fracture energy parameters for DLA mix has increased compared with A and Co mixes indicating an improvement in crack growth resistance in DLA mix. However, such difference was not statistically significant at 90% level of confidence using ANOVA. Although it was found that aging stiffens the film which increases the strength of the asphalt concrete specimens [34], the aging temperature of the specimens conditioned in this study was relatively low, so the similar film stiffening might not have occurred.
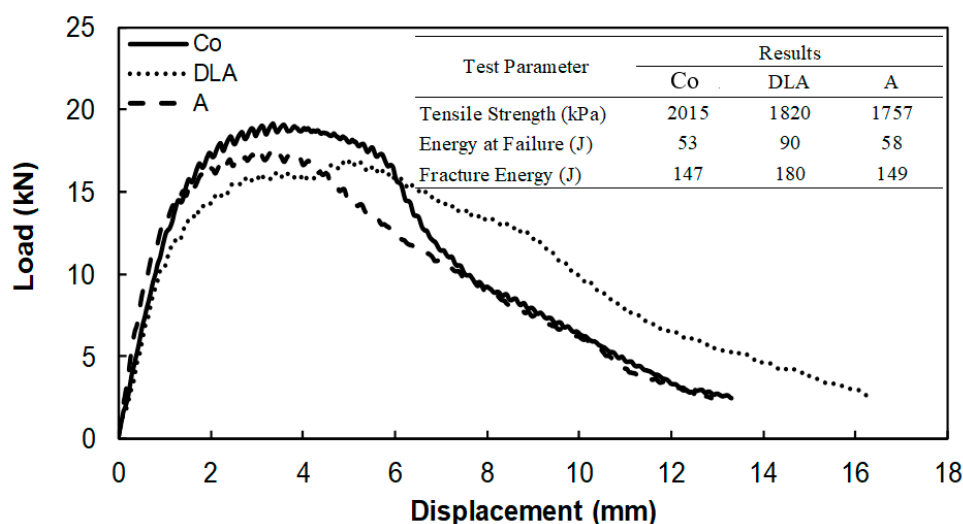

Test Parameter	Results		
	Co	DLA	A
Tensile Strength (kPa)	2015	1820	1757
Energy at Failure (J)	53	90	58
Fracture Energy (J)	147	180	149

Figure 11. Comparison of IDT test results for unconditioned mix (Co) and conditioned mixtures (DLA and A).
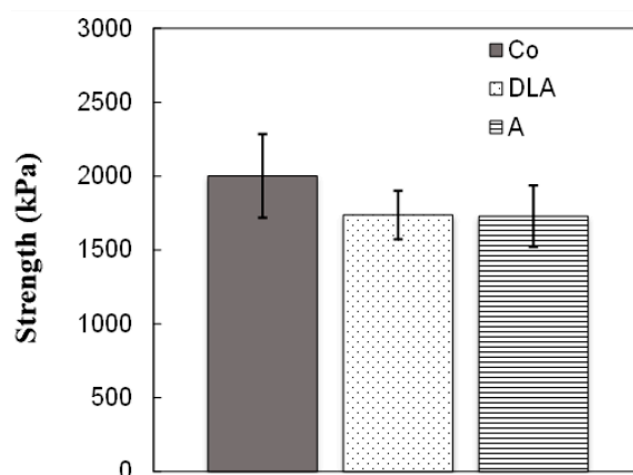
Figure 12. Indirect tensile strength values for unconditioned mix (Co) and conditioned mixtures (DLA and A).

4. Conclusions

This laboratory study attempted to experimentally measure the rejuvenation process that crumb rubber modified mixtures exhibit when subjected to dynamic traffic loads. Findings were:

1. The swelling effect of rubber particles was studied using electron microscopy images on pre- and post-blended rubber particles in asphalt cements, and it was found that the particles swelled in the range of 15.8–49.3% with those in softer asphalt indicating the largest swelling.

2. Specimens subjected to dynamic load aging has a shinier surface (richer in binder content) compared to those aged without any loading. The shiny surface of the aged sample under dynamic load was attributed to the presence of oils migrating out from crumb rubber particles over the conditioning period. Such observation may corroborate the hypothesis of this study claiming that the oily compounds are squeezed out from crumb rubber particles upon exposing the pavement to traffic loads.

3. Aged samples subjected to dynamic load (DLA) showed higher creep compliance compared to samples aged without loading (A). As mentioned above, the presence of oily compounds can provide more flexibility in behavior; the higher flexibility of DLA samples resulted in higher creep compliance compared with the A samples. This observation was also supported by statistical significance for the creep compliance values. The significance was more pronounced after 10 s of creep compliance testing. Nevertheless, it is still possible that the DLA and A samples were damaged given the increase in the air void content after conditioning causing the specimens to be more compliant. However, the IDTs showed no statistical difference between the strength of the conditioned and unconditioned specimens; therefore, it might be unlikely that the differences in the compliance was resulted from the damaged specimens.

4. The IDT strength test results did not show a difference between the various conditions; however, the average fracture energy parameters for the DLA mix were higher compared with the A mixture indicating an improvement in cracking and growth resistance. Based on the limited number of tests, such difference was not statistically significant at a 90% level of confidence.

The preliminary results of this study are promising, but more work and expanded testing program is recommended as a follow up effort. The immediate future testing should include conventional and asphalt rubber modified mixtures, consideration of confined testing to accommodate the open and gap gradations found in asphalt rubber mixtures, aging temperature and duration, and additional surface image analysis.

References

1. Glover, C.J.; Davison, R.R.; Domke, C.H.; Ruan, Y.; Juristyarini, P.; Knorr, D.B.; Jung, S.H. Development of a new method for assessing asphalt binder durability with field validation. *Tex. Dept Transp.* **2005**, *1872*, 1–334.
2. Lee, S.-J.; Amirkhanian, S.N.; Shatanawi, K.; Kim, K.W. Short-term aging characterization of asphalt binders using gel permeation chromatography and selected Superpave binder tests. *Constr. Build. Mater.* **2008**, *22*, 2220–2227. [CrossRef]
3. Roberts, F.L.; Kandhal, P.S.; Brown, E.R.; Lee, D.; Kennedy, T.W. *Hot Mix Asphalt Materials, Mixture Design and Construction*; NAPA Education Foundation: Lanham, MD, USA, 1996.
4. Morian, N.; Hajj, E.; Glover, C.; Sebaaly, P. Oxidative aging of asphalt binders in hot-mix asphalt mixtures. *Transp. Res. Rec. J. Transp. Res. Board.* **2011**, 107–116. [CrossRef]
5. Bell, C.A. *Summary Report on Aging of Asphalt-Aggregate Systems*; Strategic Highway Research Program; National Research Council: Washington, DC, USA, 1989.
6. Abbas, A.; Choi, B.C.; Masad, E.; Papagiannakis, T. The influence of laboratory aging method on the rheological properties of asphalt binders. *J. Test. Eval.* **2002**, *30*, 171–176.
7. Airey, G.D. State of the art report on ageing test methods for bituminous pavement materials. *Int. J. Pavement Eng.* **2003**, *4*, 165–176. [CrossRef]
8. Lesueur, D. The colloidal structure of bitumen: Consequences on the rheology and on the mechanisms of bitumen modification. *Adv. Colloid Interface Sci.* **2009**, *145*, 42–82. [CrossRef] [PubMed]
9. Vallerga, B.A. Pavement deficiencies related to asphalt durability. *Assoc. Asph. Paving Technol. Proc.* **1981**, *50*, 481–491.
10. Heitzman, M.A. *State of the Practice: Design and Construction of Asphalt Paving Materials with Crumb-Rubber Modifier*; Final Report; No. PB-92-203900/XAB; FHWA/SA–92/022; Federal Highway Administration, Office of Engineering: Washington, DC, USA, 1992.
11. Samuel, C.; Mohammad, L.; Abadie, C. *Evaluation of Field Projects Using Crumb Rubber Modified Asphaltic Concrete*; No. FHWA/LA. 04/393; Louisiana Transportation Research Center: Baton Rouge, LA, USA, 2007.
12. Irfan, M.; Ali, Y.; Ahmed, S.; Hafeez, I. Performance evaluation of crumb rubber-modified asphalt mixtures based on laboratory and field investigations. *Arab. J. Sci. Eng.* **2018**, *43*, 1795–1806. [CrossRef]
13. Cao, W. Study on properties of recycled tire rubber modified asphalt mixtures using dry process. *Constr. Build. Mater.* **2007**, *21*, 1011–1015. [CrossRef]
14. Presti, D.L. Recycled tyre rubber modified bitumens for road asphalt mixtures: A literature review. *Constr. Build. Mater.* **2013**, *49*, 863–881. [CrossRef]
15. Palit, S.K.; Reddy, K.S.; Pandey, B.B. Laboratory evaluation of crumb rubber modified asphalt mixes. *J. Mater. Civ. Eng.* **2004**, *16*, 45–53. [CrossRef]
16. Navarro, F.J.; Partal, P.; Martınez-Boza, F.; Gallegos, C. Thermo-rheological behaviour and storage stability of ground tire rubber-modified bitumens. *Fuel* **2004**, *83*, 2041–2049. [CrossRef]
17. Huang, B.; Mohammad, L.; Graves, P.; Abadie, C. Louisiana experience with crumb rubber-modified hot-mix asphalt pavement. *Transp. Res. Rec. J. Transp. Res. Board.* **2002**, *1789*, 1–13. [CrossRef]
18. Kutay, M.E.; Ozturk, H.I. Investigation of moisture dissipation in foam-based warm mix asphalt using synchrotron-based X-ray microtomography. *J. Mater. Civ. Eng.* **2011**, *24*, 674–683. [CrossRef]
19. Medina, J.R.; Underwood, B.S. Micromechanical shear modulus modeling of activated crumb rubber modified asphalt cements. *Constr. Build. Mater.* **2017**, *150*, 56–65. [CrossRef]
20. Dong, D.; Huang, X.; Li, X.; Zhang, L. Swelling process of rubber in asphalt and its effect on the structure and properties of rubber and asphalt. *Constr. Build. Mater.* **2012**, *29*, 316–322. [CrossRef]
21. Bahia, H.U.; Davies, R. Effect of crumb rubber modifiers (CRM) on performance related properties of asphalt binders. *Asph. Paving Technol.* **1994**, *63*, 414.
22. Xiao, F.; Putman, B.J.; Amirkhanian, S.N. Laboratory investigation of dimensional changes of crumb rubber reacting with asphalt binder. *Proc. Asph. Rubber* **2006**, *82*, 71.

23. Way, G.B.; Kaloush, K.; Biligiri, K.P. Asphalt-rubber standard practice guide—An overview. In Proceedings of the Asphalt Rubber 2012, München, Germany, 23–26 October 2012; pp. 23–40.

24. Bell, C.A.; AbWahab, Y.; Cristi, M.E.; Sosnovske, D. *Selection of Laboratory Aging Procedures for Asphalt-Aggregate Mixtures*; Strategic Highway Research Program; National Research Council: Washington, DC, USA, 1994.

25. Lee, M.G.; Tia, M.; Ruth, B.E.; Page, G.C. Comparison between the aging processes for asphalt mixtures and those for asphalt binders. In *Progress of Superpave (Superior Performing Asphalt Pavement): Evaluation and Implementation*; Jester, R., Ed.; ASTM International: West Conshohocken, PA, USA, 1997; pp. 126–134.

26. Romero, P.; Roque, R. Evaluation of long-term oven aging of asphalt mixtures (AASHTO PP2) on superpave thermal cracking performance predictions. In *Progress of Superpave (Superior Performing Asphalt Pavement): Evaluation and Implementation*; Jester, R., Ed.; ASTM International: West Conshohocken, PA, USA, 1997; pp. 151–168.

27. Piérard, N.; Vanelstraete, A. Developing a test method for the accelerated ageing of bituminous mixtures in the laboratory. In *Advanced Testing and Characterization of Bituminous Materials*; Loizos, A., Partl, M.N., Scarpas, T., Al-Qadi, I.L., Eds.; Taylor & Francis Group: London, UK, 2009; pp. 163–171.

28. De la Roche, C.; Van de Ven, M.; Gabet, T.; Dubois, V.; Grenfell, J.; Porot, L. Development of a laboratory bituminous mixtures ageing protocol. In *Advanced Testing and Characterization of Bituminous Materials*; Loizos, A., Partl, M.N., Scarpas, T., Al-Qadi, I.L., Eds.; Taylor & Francis Group: London, UK, 2009; pp. 331–345.

29. Crucho, J.; Picado-Santos, L.; Neves, J.; Capitão, S.; Al-Qadi, I.L. Tecnico accelerated ageing (TEAGE)—A new laboratory approach for bituminous mixture ageing simulation. *Int. J. Pavement Eng.* **2020**, *21*, 753–765. [CrossRef]

30. Das, P.K.; Baaj, H.; Kringos, N.; Tighe, S. Coupling of oxidative ageing and moisture damage in asphalt mixtures. *Road Mater. Pavement Des.* **2015**, *16* (Suppl. 1), 265–279. [CrossRef]

31. Zborowski, A.; Kaloush, K.E. A fracture energy approach to model the thermal cracking performance of asphalt rubber mixtures. *Road Mater. Pavement Des.* **2011**, *12*, 377–395. [CrossRef]

32. Roscoe, R. The viscosity of suspensions of rigid spheres. *Br. J. Appl. Phys.* **1952**, *3*, 267. [CrossRef]

33. Kutay, M.E.; Ozturk, H. Internal structure characteristics of crumb rubber modified asphalt binders: An analysis using 3D X-ray microtomography imaging. In Proceedings of the Asphalt Rubber Conference, Munich, Germany, 23–26 October 2012; pp. 1–10.

34. Islam, M.R.; Hossain, M.I.; Tarefder, R.A. A study of asphalt aging using Indirect Tensile Strength test. *Constr. Build. Mater.* **2015**, *95*, 218–223. [CrossRef]